

A Comprehensive Characterization of Commercial Conductive Yarns for Smart Textile Applications

Aftab Ahmed ¹(✉)*, Mira Haberfellner ¹*, Federica Morandi ¹, Thomas Preindl ¹,
Andreas Pointner ¹, Anita Vogl ², Cohen Nitzan ¹, Andrea Gasparella ¹, Niko Mützenrieder ¹, and Michael Haller ^{1,*}

¹ Faculty of Engineering, Free University of Bozen-Bolzano

² University of Applied Sciences Upper Austria

* Both authors contributed equally to this work
aftab.ahmed@student.unibz.it

Abstract. The development of conductive yarns is growing rapidly due to their use in wearable electronic textiles for sensing, heating, and energy storage applications. These yarns can be integrated into fabrics using traditional textile fabrication techniques such as Embroidery, weaving, and Knitting. Their structural properties play a crucial role in the processability of fabrication techniques and atmospheric conditions, abrasion resistance, and sweat on the overall performance of the conductive yarn. However, an efficient evaluation of these properties of commercial conductive yarns remains limited. This work focuses on characterizing 15 commercially available conductive yarns with varying structures, materials, and fabrication techniques to evaluate structural properties, processability in embroidery, and abrasion resistance. Structural properties such as thick/thin places and hairiness were measured, along with their effects during embroidery. Changes in resistance due to abrasion were also evaluated to predict variations in electrical performance during wear. Additional tests were conducted in a climate chamber with temperature variations from 5 °C to 45 °C and a thermal manikin operating in dry and wet conditions to check the real-time effect during wearability. Highly twisted yarns with low hairiness demonstrated superior processability and resilience during embroidery and abrasion tests, maintaining stable electrical properties. In contrast, lower-twist yarns frequently experienced breakages and entanglements due to reduced structural integrity. Most materials displayed consistent resistance across varying conditions, ensuring reliability for wearable applications. However, one material exhibited significant variability, highlighting repeatability issues. Resistance changes during wet conditions depended on the sample's proximity to sweating pores. These findings provide a framework for selecting and characterizing conductive yarns, offering valuable insights for their integration into textile-based wearables and advancing the field of smart textiles.

Keywords: Conductive yarns, Wearable textiles, Smart textiles

1 Introduction

Smart textiles have the potential to transform how we interact with computing systems by shifting interactions to a more intimate level through direct body contact. Unlike conventional devices that require explicit actions like tapping, typing, or speaking, smart textiles offer a more natural and easy interaction by responding to the body's natural movements and gestures. For instance, health-monitoring garments embedded with sensors can autonomously track vital signs like heart rate and respiration, requiring no user intervention [1]. Similarly, smart gloves knitted with conductive yarns can recognize hand movements, allowing users to control digital devices through natural hand movements [2]. As integral components of smart textiles, conductive yarns play a key role in shaping a new way for wearable technology, where the boundaries between fabric and device blend.

For centuries, traditional yarns have been the backbone of weaving, knitting, and sewing, developed through a legacy of intricate craftsmanship and material understanding. Expanding on this base, conductive yarns bring in new elements such as conductive polymers, graphene, carbon nanotubes, and metals [3]. Although these materials provide useful electrical properties, they also bring about specific difficulties in terms of processing and integration [4]. A crucial aspect involves assessing the characteristics and suitability of commercially available conductive yarns for textile applications. Prior studies, like those by Shahood et al., highlight how mechanical stresses (twisting, friction, bending), chemical influences, water exposure, and thermal stress can affect the durability and functionality of conductive yarns [5, 6]. Mareen N. Warncke et al. investigated the washing fastness of silver-plated conductive yarns [7]. Similarly, Yu Chen et al. conducted an electrochemical characterization of commercially available conductive yarns [8], while R.K. Raji et al. classified conductive yarns based on their types and conductivity ranges [9]. Johannes Mersch et al. worked on integrated temperature and position sensors in a shape-memory-driven soft actuator [10]. Additionally, Hao et al. explored using silver filaments for heating textile applications [11]. Yet, there are still gaps in comprehending how these yarns behave when subjected to traditional textile techniques like sewing, embroidery, weaving, and knitting, which are their intended applications.

This article categorizes conductive yarns based on their manufacturing methods, focusing on types best suited for embroidered sensors in smart textiles. Given the prohibitive cost and limited accessibility of specialized testing equipment, a practical approach is developed for evaluating the characteristics of conductive yarns using accessible tools. This method focuses on traditional textile parameters, enhancing the usability of testing and providing key insights into yarn suitability for specific applications, ultimately improving selection precision and performance reliability in smart textiles.

The methodology begins by investigating the processes involved in yarn fabrication to understand how yarns gain conductivity. In this paper, 15 commercially available conductive yarns were chosen from this classification and conducted thorough testing on each to assess their appropriateness for embroidery. The evaluation considers important characteristics such as variations in yarn thickness, and hairiness, all of which impact the yarn's suitability for use in embroidery machines. Further, the chosen yarns

were tested for durability, specifically examining their resistance to abrasion and ability to maintain electrical stability in diverse environmental conditions, such as changes in temperature and humidity. Furthermore, the yarns were assessed how well the yarns performed in real-life scenarios by simulating their usage on a manikin to evaluate their practicality. This evaluation approach merges traditional textile standards with advanced performance measurements, empowering informed decision-making when choosing conductive yarns for smart textile applications. The contributions of this paper are summarized as follows:

- After evaluating different potential threads, numerous tests were conducted to identify the most suitable candidates, which were then selected for further testing.
- Initially, the yarns were examined using a microscope for in-depth analysis to assess attributes such as thickness variations and hairiness. These test outcomes played a pivotal role in selecting the final candidates for the prototype.
- Finally, additional samples were created and tested in a temperature chamber and a thermal manikin to simulate heat exchange between the human body and the environment.
- By establishing a structured assessment framework for conductive yarns, this method enhances the field and contributes to the creation of reliable and efficient smart textile products.

2 Materials and Methods

In the first experiment, 15 commercial conductive yarns were selected (cf. **Fig. 1** and **Table 1**). Both the figure and the table summarize key details of these yarns, such as their type, quantity, material, and resistance per unit length.

The construction of all categories of yarns, including spun, plied spun and core spun (Bart-Francis and Schoeller), multifilament (Madeira HC 40, Shieldex, King Smart), and twisted filaments (Amann yarns, Clever Tex. In the spun yarn category, blends of polyester and Merino wool with stainless steel (inox) are common with spun, plied, and core spun techniques. In the category of twisted filaments, yarns are a blend of materials like polyamide or polyester with silver, copper, and stainless steel, showing a wide range of resistance, from relatively low to much higher values depending on the yarn's specific structure and materials. The table shows that all yarns include spun, multifilament, and twisted filament yarns with different parameters given by manufacturers. The performance of conductive yarns in smart textile applications is significantly influenced by their structure, which determines their functionality and versatility. These conductive yarns are selected for their end use in different smart textile applications. It is essential for researchers to thoroughly understand the structure and properties of each type of conductive yarn to tailor their materials and create cutting-edge and efficient smart textile solutions [12].

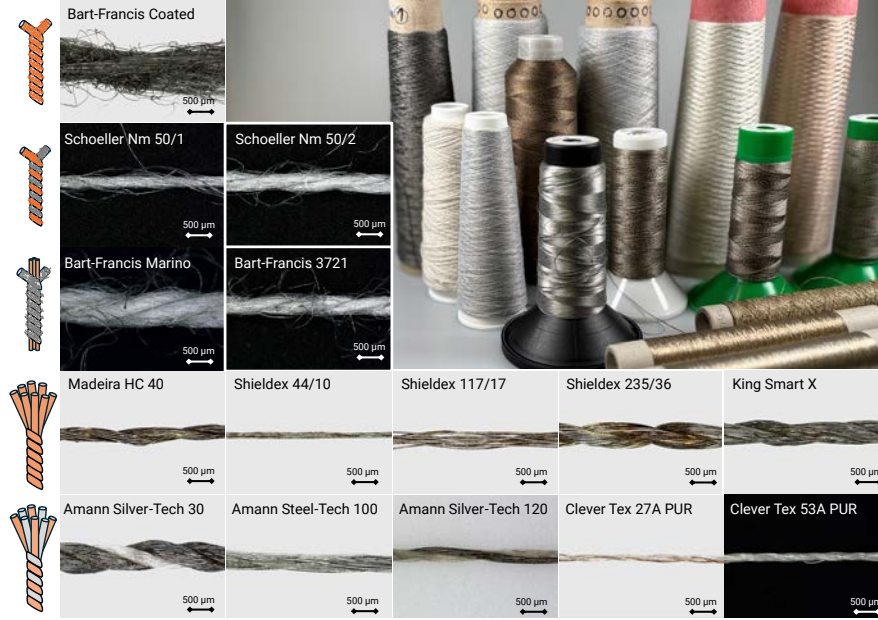






Fig. 1. Categorized all yarns by fabrication method, including coated spun, spun using conductive staples, core-spun yarns, and the two versions of twisted filaments.

The physical and mechanical properties of the resulting yarns are determined by how their components are arranged, with the spinning angle playing a significant role in the final structure [13]. Smart textiles can be used for applications such as antibacterial properties, and strain/pressure-sensing. The structure of conductive yarns significantly influences their electrical conductivity, flexibility, and durability. The arrangement and distribution of conductive fibers within the yarn structure play a crucial role in determining the yarn's characteristics. Metallic (Ag, Cu, etc.) or nonmetallic (conductive polymers, carbon-based materials) conductive fibers are also possible for the yarn. Even distribution of conductive fibers throughout the yarn results in consistent conductivity along its entire length. Conductive fibers forming clusters or gaps within the yarn can decrease its conductivity. Yarn stability, strength, stretchability, and flexibility are all enhanced via twisting. However, the excess twist may cause the conductive fibers to break or lose some of their electrical conductivity. The yarn's overall composition, the conductive fibers' diameter and thickness, and other factors further influence the qualities [14].

This study explores how different fabrication processes and yarn parameters impact the performance and usability of conductive yarns. It also investigates which yarn parameters, like hairiness, thickness variations, and durability, are most suitable for further smart textile applications.

Table 1: This table provides a detailed comparison of various yarn types used in our experiments, listing their characteristics such as yarn type, yarn count, base material, and resistance per meter, which are given by manufacturers.

Construction Method	Name	Yarn Type	Yarn Count	Base Material	Resistance
	Bart-Francis Coated	2 ply	-		67 Ω /m
	Schoeller (Nm 50/1)	Single	200 dtex	Polyester/Inox	1.6 M Ω /m
	Schoeller (Nm 50/2)	2 ply	200 dtex	Polyester/Inox	2.9 k Ω /m
	Bart-Francis Marino	3 ply	-	Merino/Inox	307 Ω /m
	Bart-Francis 3721	2 ply	-	Polyester/Inox	3 k Ω /m
	Madeira HC 40	2 ply	234 dtex	Polyamide coated with Ag	<300 Ω /m
	Shieldex 44/10	Single	44 dtex	Polyamide coated with Ag	\leq 4 k Ω /m
	Shieldex 117/17	Single	117 dtex	Polyamide coated with Ag	<1.5 k Ω /m
	Shieldex 235/36	2 ply	235 dtex	Polyamide coated with Ag	\leq 2.5 k Ω /m
	King Smart X	3 ply	335 dtex	Nylon coated with Ag	10 Ω /m
	Amann Silver-Tech 30	3 ply	960 dtex	Polyamide/Polyester/Ag	<85 Ω /m
	Amann Steel-Tech 100	3 ply	330 dtex	Stainless Steel/Polyester	<110 Ω /m
	Amann Silver-Tech 120	3 ply	270 dtex	Polyamide/Polyester/Ag	<530 Ω /m
	Clever Tex 27A PUR	2 ply	370 dtex	Polyester/Cu-Zn	14.65 Ω /m
	Clever Tex 53A PUR	2 ply	600 dtex	Polyester/Cu-Ag	7.48 Ω /m

2.1 Apparatus & Design

A Leica DVM6 microscope was used to examine the conductive yarns' structure, cf. **Fig. 2** (A), comparing each measurement to the average diameter, which was calculated from a length of 8 cm. The microscope recordings were utilized to classify the different yarns based on their structure. Consequently, all yarns were identified as twines, composed of spun or filament yarns. These yarns were either fully or partially conductive, often combined with another material.

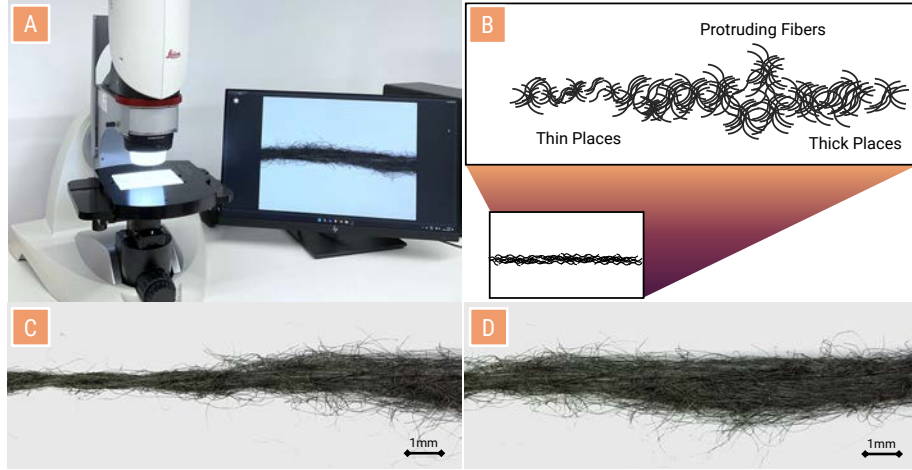


Fig. 2. A yarn (A) often comprises different fibers, with some protruding fibers (B). But also, thin (C) and thick (D) places can be observed, resulting in a less smooth fabric.

The average thick and thin places (cf. **Fig. 2, B**) were calculated by measuring the yarn's diameter along its length and identifying deviations from the average. A thick place was identified when the diameter at a point exceeded the entire length by 50%, while a thin place was noted when the diameter fell 50% below the whole length. For each section of yarn, thick and thin places were manually counted to determine how often the diameter surpassed or dropped below these thresholds. These were only measured for the spun and twisted filaments, as no thin and thick places were observed in multifilament yarns. After measuring the entire yarn sample (8 cm), the total number of thick and thin places per unit of length was calculated.

Hairiness

Yarn hairiness, which refers to the number of excess length fibers that stick out from a yarn, is a key factor in assessing yarn quality. This characteristic has a notable impact on the performance of yarn, especially in conductive yarns, affecting their processing, conductivity, and mechanical strength [15].



Fig. 3. Examples of hairiness of different yarn samples include Bart-Francis Coated (A), Schoeller, Nm 50/2 (B), and Bart-Francis Marino (C).

In this experiment, the number and average length of protruding fibers were measured using a microscope equipped with built-in software (Leica Microscope Imaging). The software enabled accurate tracking and counting of yarn hairs for visual inspection and length measurement. In contrast to traditional manual methods [16], this approach provides ease of use and higher accuracy in capturing yarn hairiness details. The software enables users to trace yarn hairs in both straight and curved paths. This feature ensures precise measurement of each hair's length, even when it follows a non-linear path, addressing a limitation of traditional methods that assume straight fibers or use measurements along a single axis. With an easy click-to-count feature, it can quickly tag each hair by clicking on its location, generating a number at the exact location. Automated counting removes inaccuracies associated with manual counting and speeds up the process of collecting data. This process enables easy and repeatable counting, ensuring the method is accessible to users without the need for extensive training. This method achieves results comparable to traditional measurement tools but with fewer steps and improved user interface support. By simplifying procedures, the methodology offers accurate hairiness data and easy replicability, benefiting other researchers in textile studies.

To quantify the hairiness, 10 specimens of yarn, each 8 cm in length, were used. To improve contrast during imaging, different colored background surfaces were used due to the varying colors of the yarn samples. The choice of background was critical in clearly distinguishing the yarn from the protruding fibers, enabling accurate measurement. Also, the number of fibers extending from the yarn's surface is counted, which provides a hairiness index cf. [17], a measure of the yarn's fuzziness that can be further expressed as

$$\text{Hairiness index} = \frac{\text{total length of protruding fibers}}{\text{length of yarn measured}} \quad (1)$$

The hairiness index represents the ratio between the total length of the fibers that stick out from the surface of the yarn and the actual length of the yarn section being analyzed. A higher hairiness index suggests that more fibers protrude from the yarn, indicating a fuzzier or hairier texture. Conversely, a lower hairiness index suggests fewer fibers protrude, meaning the yarn has a smoother surface. Summarizing, this measurement helps in assessing the quality, appearance, and performance of the yarn. characteristics of the yarn, especially in applications where smoothness or surface texture is important.

2.2 Apparatus & Design

In the second experiment, embroidery was chosen to assess the yarns' processability, given their efficiency, minimal material requirements, and ease of prototyping. Various textile structures were tested for embroidery suitability using a Tajima Sai (MDP-S0801C) machine. Synthetic laminated fabric was selected as the base material due to its thickness, which facilitated further tests and visual inspection. Embroidery was performed at a uniform speed of 500 RPM with a 0.40 mm stitch length. The upper thread,

visible on the fabric's surface, passed through the needle, while the lower thread, wound on a bobbin, secured the stitches. A highly twisted 100% lyocell yarn was used for the lower thread, ensuring a strong connection. The upper thread underwent more stress due to its passage through tensioning devices and repeated needle movements.

After performing the first experiment, the remaining six yarns (Madeira HC 40, Schoeller (Nm 50/2), Bart-Francis 3721, Amann Silver-Tech 120, Clever Tex 27A PUR, and Clever Tex 53A PUR) were selected for embroidery with four different 2×2 cm patterns, as shown in **Fig. 4**, including four different types of patterns, which are mostly used for textile fabrications.

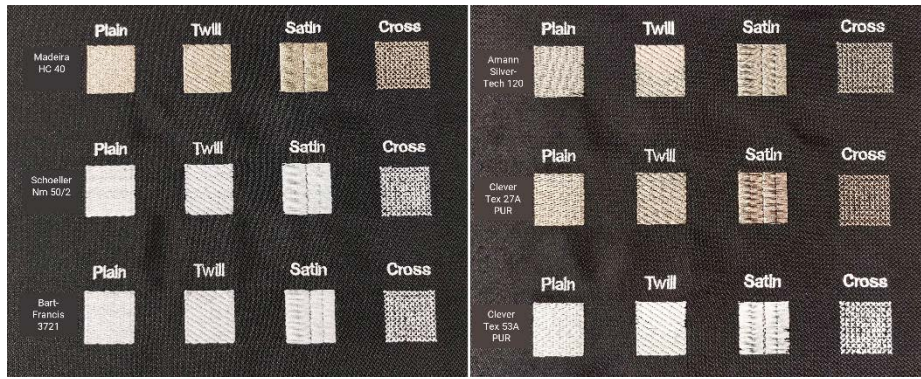


Fig. 4. All the presented yarns, which could be easily implemented as upper thread, include Madeira HC 40, Schoeller, NM 50/2, Bart-Francis 3721, Amann Silver-Tech 120, Clever Tex 27A PUR, and Clever Tex 53A PUR.

By continuing the above experiment, the abrasion resistance was also measured in embroidered textile samples, particularly focusing on smart textiles that incorporate conductive yarns. Abrasion resistance refers to a material's ability to maintain its structural and functional properties when subjected to friction or wear. This property is crucial in applications like clothing, shoes, machine parts, and wearable solutions, where frequent friction can degrade the material's performance. For smart textiles, the durability of conductive yarns is particularly important, as friction can negatively impact the material's functionality, affecting the lifespan and stability of the product. Understanding and improving abrasion resistance can guide manufacturers in enhancing product quality and help consumers select durable, high-performance products. To conduct this experiment, a custom-built CNC router was used (**Fig. 5**). The CNC router, controlled by ArtSoft Mach4 CNC Control Software (v4.2.0) on a Windows 10 PC, was used to simulate friction on the textile samples. The system was equipped with a Sauter CP single-point load cell, which acted as the actuator. Data from the load cell was sampled at 80 Hz using an ADS 1231 24-bit Delta-Sigma converter. To manage the sampling process and data collection, an Ada-fruit ESP32 microcontroller was utilized, which also communicated with Mach4 via RS232 to synchronize the testing procedure based on feedback from the textile samples.

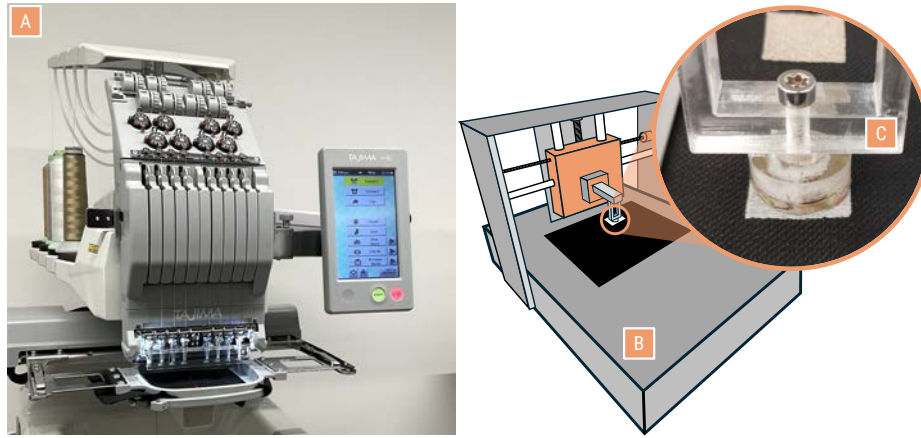


Fig. 5. *Tajima Sai (MDP-S0801C) embroidery machine and a custom-built CNC router for testing abrasion on the samples.*

Standardized methods, such as OENORM EN ISO 12947-1 using the Martindale tester, are widely used for abrasion testing. However, as the field of smart textiles is inherently multidisciplinary, involving researchers from both textile and non-textile domains, access to specialized textile testing equipment may not always be feasible. In such contexts, alternative approaches, like the use of a built-in machine, provide an accessible and adaptable solution. This study demonstrates how such methods can still produce meaningful and reliable results, encouraging broader participation in smart textile research without the constraint of limited access to standardized equipment.

During the experiment, parameters such as applied force, abrasion speed, abrasion radius, and the number of rotations were specified. These parameters were defined in a G-code file, which was then uploaded to the machine to evaluate the abrasion resistance and performance of the embroidered textiles under simulated wear conditions. To analyze their abrasion resistance and performance, the samples were securely mounted on the testing machine's sample holder to prevent surface distortions and maintain consistent contact for accurate testing results. The test parameters were established, specifying the force as 2 N for the first cycle, 3 N for the second cycle, and 4 N for the third cycle, along with the type of grinding head, rotation speed, and pattern. These variables were meticulously chosen to closely mimic actual friction and wear conditions, ensuring a realistic simulation in the experiment. Subsequently, the grinding head (using sandpaper with a 320-grit number and a diameter of 2 cm) was applied to the material surface with a required force and a feed rate of 700 mm/m, simulating the abrasion the material might face in practical use. After completing 30 cycles in the first phase, 50 cycles in the second, and 70 cycles in the third phase, the surface changes of the material under a microscope were analyzed. In addition to visual inspection, the electrical resistance was also measured to quantify the wear of the material and evaluate the performance of the sensors. Lastly, the data analysis concentrated on assessing the abrasion

resistance of each material, specifically looking at resistance changes over time and visible surface damage to evaluate the materials' conductivity under mechanical stress.

2.3 Apparatus & Design

In the next experiment, to determine whether the embroidered samples would yield reliable measurement results under varying conditions, this included testing for large temperature fluctuations and examining whether the electrical properties changed significantly when the sample was affected.

To perform this experiment, embroidered samples measuring 2 x 2 cm with plain structure (due to overall performance, as confirmed by the abrasion test results) were prepared. By performing the previous experiments, the yarn Schoeller NM 50/2 was removed due to its fabrication performance. Five samples per yarn were placed in an Ange-lantoni DM340 climate chamber where controlled temperature steps were imposed, ranging from 5 °C to 45 °C. The samples were connected to a DAQ970A Keysight acquisition system (2-wire resistance) using crocodile clips, and data was logged with a 10s-time resolution. A pt100 RTD was also placed inside the climate chamber close to the samples for reference.

Additionally, a Newton thermal manikin was used to simulate heat exchange between the human body and the environment and investigate the behavior of such samples as wearable devices when sweating is triggered or not. In this experiment, Normal boundary conditions were set. Temperature and sweat rate were used to control the manikin, and the heat flux measured by the manikin was used as control feedback. Measurements were conducted in two steps. First, a constant temperature of 35 °C was set for the involved body segments, and the manikin was operated in dry mode. After steady-state conditions were reached, the samples' resistance was monitored for 100 min. Then, sweating was activated with a flow rate of 1000 ml h⁻¹ m⁻², while keeping the same skin temperature. After approximately 30 min, water was uniformly spread throughout the arm, and samples reached a uniform soaking level; an additional 60 min of data acquisition was performed. During the experiment, the manikin was covered with a specific suit designed to spread sweat all over the body, and textile samples, with dimensions 2x6 cm, were fixed on a portion of the manikin's arm using elastic bands. Skin temperature, heat flux, the resistance measured from the textiles, and environmental conditions were monitored throughout the whole duration of the test. Skin temperature, heat flux, and environmental conditions were retrieved from the manikin, while resistance was measured using the DAQ970A Keysight acquisition system described above.

3 Results

3.1 Thick Places

Fig. 6 summarizes the average number of thick places in the spun yarns. Among the chosen yarns, Bart-Francis Marino exhibits more thick places (around 2), suggesting irregularities in the yarn structure, potentially due to the higher fiber content or

processing technique. This indicates that the fiber distribution in Bart-Francis Marino may be irregular, resulting in areas where the yarn is thicker. Bart-Francis Coated exhibits a comparably elevated frequency of thick places, equivalent to Bart-Francis Marino yarn, with an average of 2 thick places per unit length. This indicates a comparable pattern of structural irregularity, potentially due to the fiber's uneven coating or inadequate material tension. In textile manufacturing processes such as embroidery, thick areas can lead to problems, as these regions may be stuck in the needle hole, causing yarn breakage, disrupting the embroidery process, and disrupting conductive pathways. Conversely, Bart-Francis 3721 and Schoeller (Nm 50/2) do not exhibit many thick places, averaging approximately 1 and 1.5, respectively. The results indicate a more uniform fiber structure in these yarns relative to others, exhibiting fewer impurities, which may result in fewer complications during embroidery and more mechanical stability. The Schoeller (Nm 50/1) yarn demonstrates the least thick places (around 0.5), indicating a relatively smooth and uniform yarn structure with minimal coarse cross-sectional areas. This lower level of irregularity could result in more reliable performance in further processes.

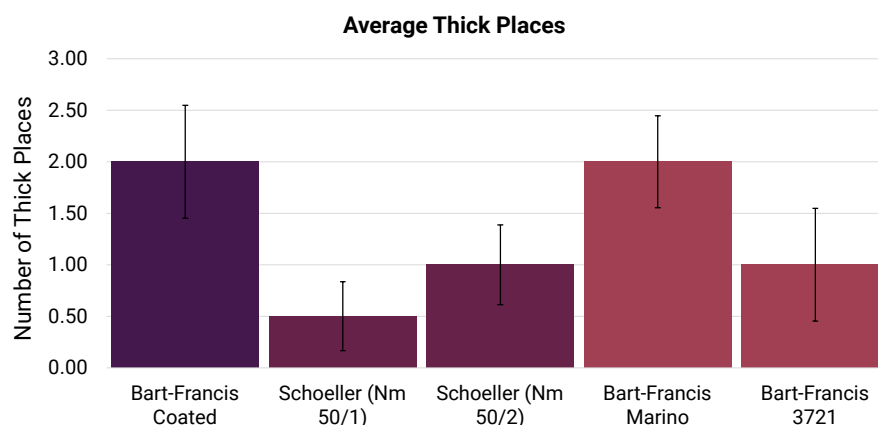


Fig. 6. The chart displays the average number of thick places in spun yarns, showcasing variations among Schoeller (Nm 50/1), Schoeller (Nm 50/2), Bart-Francis Marino, Bart-Francis 3721, and Bart-Francis Coated.

Regarding thin places, only Schoeller (Nm 50/1) and Bart-Francis Coated showed very few places. This indicates that while these yarns exhibit some degree of thickness variation, they maintain a relatively stable structure with minimal areas where the yarn becomes finer than the overall cross-section of the yarn. However, even minor thin places may cause weaknesses during embroidery, as thinner sections may not hold up well under tension by passing through guiders and tensioners potentially leading to yarn breakage. Interestingly, no significant thick or thin places were observed in the multi-filament and twisted filaments, suggesting that these yarn types tend to have a more

uniform structure. However, in Amann Steel-tech 100 multifilament yarn, a notable number of entanglements were observed throughout its length. This could be due to the rigidity of the yarn or improper winding during the manufacturing process, potentially leading to localized areas of fiber entanglement that may affect yarn performance, particularly regarding mechanical behavior and handling.

The presence of thick and thin places across the different yarns highlights the importance of material consistency in textile processes. Higher levels of these impurities can impact not only the yarn's mechanical performance but also its usability in applications like embroidery, where the yarn must pass smoothly through the needle without causing damage or interruptions.

3.2 Hairiness

Fig. 7 provides an overview of the number of hairs for the different yarns as well as the average length of the hairiness. The spun yarn Bart-Francis Coated has the highest number of protruding hairs (approx. 85), indicating a higher level of hairiness.

The increased hairiness in Bart-Francis Coated may be due to its specific construction and materials, resulting in a looser fiber structure. This can impact the yarn's performance, particularly its interactions with other materials and mechanical strength. Other spun yarns, such as Schoeller (Nm 50/1), Schoeller (Nm 50/2), and Bart-Francis Marino, exhibit moderate hairiness, with around 50 hairs per sample, indicating a relatively even fiber structure. In contrast, Bart-Francis 3721 shows significantly fewer hairs (20), likely due to its tighter structure or smoother surface. Among twisted filaments, Amann Silver-Tech 30 has very few protruding fibers, suggesting that its fabrication using polyamide, silver, and polyester creates a smoother surface. This smoothness is advantageous in applications requiring low hairiness, such as conductive yarns, where protruding fibers could negatively affect conductivity or mechanical behavior.

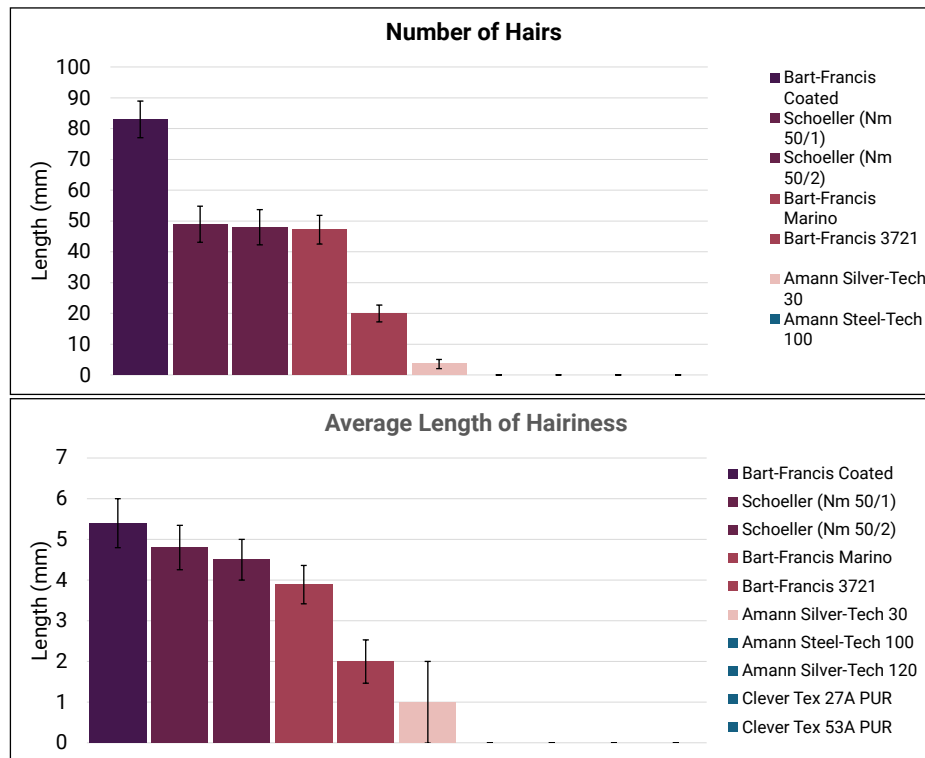


Fig. 7. Hairiness evaluation results. The number of hairs and the average length of hairiness.

Fig. 7 Illustrates the average length of protruding fibers for spun and twisted filament samples. Bart-Francis Coated shows the longest average fiber protrusion among spun yarns, reaching nearly 5.5 mm, consistent with its high number of protruding hairs. Schoeller (Nm 50/1) and Schoeller (Nm 50/2) have slightly shorter lengths, averaging around 4.5 mm, while Bart-Francis Marino averages 4 mm. Bart-Francis 3721 has the shortest fiber protrusion among spun yarns at approximately 2 mm. Twisted filaments display much lower hairiness. Amann Silver-Tech 30 shows an average protruding fiber length of 1 mm, and other twisted filaments, such as Amann Steel-Tech 100, Amann Silver-Tech 120, Clever Tex 27A PUR, and Clever Tex 53A PUR, exhibit negligible hairiness. This aligns with previous observations of minimal protruding fibers in these yarns.

These findings highlight how different yarn constructions and materials affect both the quantity and length of protruding fibers. Spun yarns, particularly Bart-Francis Coated and Schoeller varieties, exhibit longer fiber protrusions, impacting processing and performance in textile fabrication. In contrast, twisted filaments, especially those made with silver or stainless steel, have significantly shorter or no protruding fibers, enhancing conductivity, smoothness, and durability in applications. The variations in hairiness across the yarns demonstrate how their construction methods and base materials directly affect surface characteristics. The higher hairiness of spun yarns, such as

Bart-Francis Coated, and the lower hairiness of twisted filaments, like Amann Silver-Tech 30, illustrate how material composition, whether polyamide, silver, or polyester, impacts not only appearance but also functionality, particularly in technical applications like conductivity or fabric durability. **Fig. 8** (A) shows an enlarged view of yarn, with hairiness parameters measured at 2.45 mm and 2.38 mm, indicating significant hairiness. This could result in issues like increased friction or difficulties in machine processing during textile production.

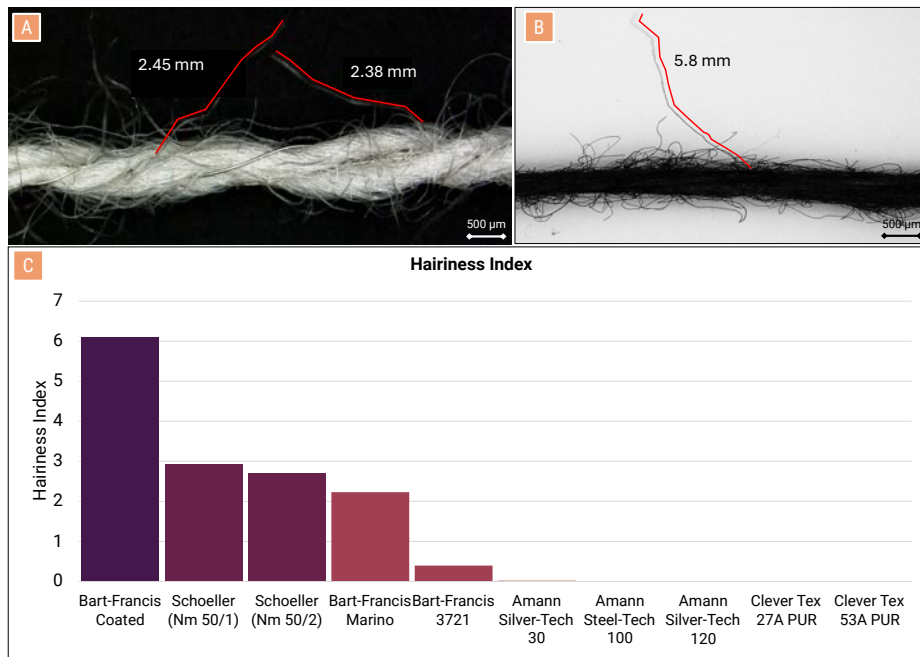


Fig. 8. The actual length along the fiber itself (A, B). An overview of the Hairiness Index shows a significantly higher value for Bart-Francis Coated (C).

Fig. 8 (B) provides an enlarged view of another yarn with reduced hairiness, with fibers measuring 1.6 mm, suggesting fewer or shorter protruding fibers compared to (A). This indicates that the yarn may perform better in smoother surface applications. The hairiness index chart in **Fig. 8** (C) presents data on various yarns, including Schoeller (Nm 50/1), Bart-Francis 3721, Amann Silver-Tech 30, and Clever Tex 53A PUR, to show differences in yarn fuzziness. Among the spun yarns, Bart-Francis Coated has a higher hairiness index, around 6, compared to the others, Schoeller (Nm 50/1), Schoeller (Nm 50/2), and Bart-Francis Marino, which range from 2 to 3. Meanwhile, Bart-Francis 3721 shows a much lower hairiness index, approximately 0.5, indicating a smoother structure. For the twisted filaments, Amann Silver-Tech 30 has a lower value of approximately 0.04, and Amann Steel-Tech 100, Amann Silver-Tech 120, Clever Tex 27A PUR, and Clever Tex 53A PUR exhibit no hairiness, reflecting their suitability for textile fabrication requiring a smooth surface.

3.3 Embroidery Process

The performance of each yarn was influenced by critical factors such as twist, fiber structure, and surface characteristics like hairiness and thickness variations. In the multifilament yarns, Shieldex 44/10, Shieldex 117/17, and Shieldex 235/36 were unsuitable for use as upper threads in embroidery due to their zero-twist structure and odd waviness, which caused instability during the embroidery process. The lack of twist compromised the yarns' structural integrity, leading to frequent failures. Similarly, Bart-Francis Coated suffered from significant breakage caused by structural entanglement, brittleness, and thick places. The presence of open, brittle short fibers in the yarn made it challenging to navigate through the needle, leading to breakage and entanglement. Both King Smart X and Amann Steel-Tech 100 faced challenges due to brittle short filaments, which hindered their passage through the needle.

Yarn Schoeller (Nm 50/1) faced frequent breakages due to zero twists and excessive hairiness, complicating the stitching process. Both Bart-Francis Marino and Bart-Francis Coated were hindered by their excessive thickness and hairiness, blocking smooth passage through the machine's needle. In the twisted filaments, Amann Silver-Tech 30 also struggled to pass through key machine components like guiders, tensioners, and needle holes due to their low twist and dispersed fibers. Conversely, yarns Schoeller (Nm 50/2) and Bart-Francis 3721 excelled as upper threads, experiencing minimal breakage attributed to occasional hairiness or thickness fluctuations along the yarn length. Yarns Madeira HC 40, Amann Silver-Tech 120, Clever Tex 27A PUR, and Clever Tex 53A PUR functioned seamlessly throughout the embroidery process. These yarns had dense structures, minimal hairiness, and consistent thickness, making them highly suitable for use as upper threads.

The findings highlight the importance of yarn characteristics such as twist, hairiness, and thickness consistency in determining their effectiveness in embroidery. Yarns with little to no twist lacked stability, leading to entanglement, breakage, and difficulty passing through machine components. Excessive hairiness and fluctuations in thickness further obstruct smooth passage through the needle and guiders, resulting in frequent thread breaks and mechanical issues. These results underscore the need to select yarns with appropriate twists, a consistent structure, and controlled hairiness for optimal embroidery performance. The friction and tension on the upper thread are significantly greater than those on the lower thread, which remains relatively stationary on the bobbin. Since the upper thread frequently contacts the fabric, needle, and machine components, it experiences more wear and is more prone to breakage. For this reason, the study focused solely on the upper thread, eliminating any yarns unsuitable for this role. The upper thread enhances efficiency, design precision, and stitching control, thereby reducing complications and optimizing the embroidery process. It also plays a key role in sensor integration, as the upper thread is more exposed to external forces like tension and friction, making it ideal for detecting subtle changes.

3.4 Abrasion

To achieve precise resistance measurements, a small setup was implemented to ensure that the same distance and pressure were maintained at both contact points. In addition, a microscope analysis was conducted to check for any optical changes (e.g., thread breakage, etc.). The behavior of conductive materials under mechanical stress, such as abrasion, is largely determined by changes in the structure of the conductive pathways. Typically, physical wear or damage disrupts these pathways, reducing the material's ability to carry electrical current and leading to an increase in resistance.

Fig. 9 provides an overview of the area resistance before abrasion and after the 1st, 2nd, and 3rd abrasion cycles for various threads with the plain stitch pattern. In analyzing textile thread performance over four cycles, Madeira HC 40 shows stable, low resistance values, with means increasing from 2.37 Ω in Cycle 0 to 3.48 Ω in Cycle 3, and a low standard deviation (SD). Bart-Francis 3721, in contrast, demonstrates considerable variability, starting at 425.56 Ω (SD = 37.26) in Cycle 0 and spiking to 1296.3 Ω (SD = 277.16) by Cycle 3, indicating substantial fluctuation across cycles caused by the high hairiness, which was measured in the previous experiment. Clever Tex 27A PUR, on the other side, shows moderate resistance, increasing from 11.56 Ω in Cycle 0 to 14.81 Ω in Cycle 3, with relatively stable SD values around 2.1 to 2.3. Schoeller (NM 50/2) maintains high resistance values, starting at 563.33 Ω (SD = 101.5) and reaching 951.85 Ω (SD = 36.66) in Cycle 3, indicating less consistency in performance. Lastly, Amann Silver Tech 120 shows again moderate, consistent resistance values, rising from 23.52 Ω in Cycle 0 to 31.11 Ω in Cycle 3, with minimal SD, indicating stability across cycles. This data underscores varying stability and performance trends across different thread materials.

In contrast, continuous filament yarns, which are made from long, unbroken strands, tend to have a more uniform structure, leading to more consistent resistance readings, as observed with Madeira HC40, Amann Silver Tech 120, Clever Tex 27A PUR, and Clever Tex 53A PUR. Further, using Madeira HC 40, a drop in resistance was noted, which may have resulted from fiber compression or realignment, improving the conductive pathways by reducing contact resistance and increasing surface contact.

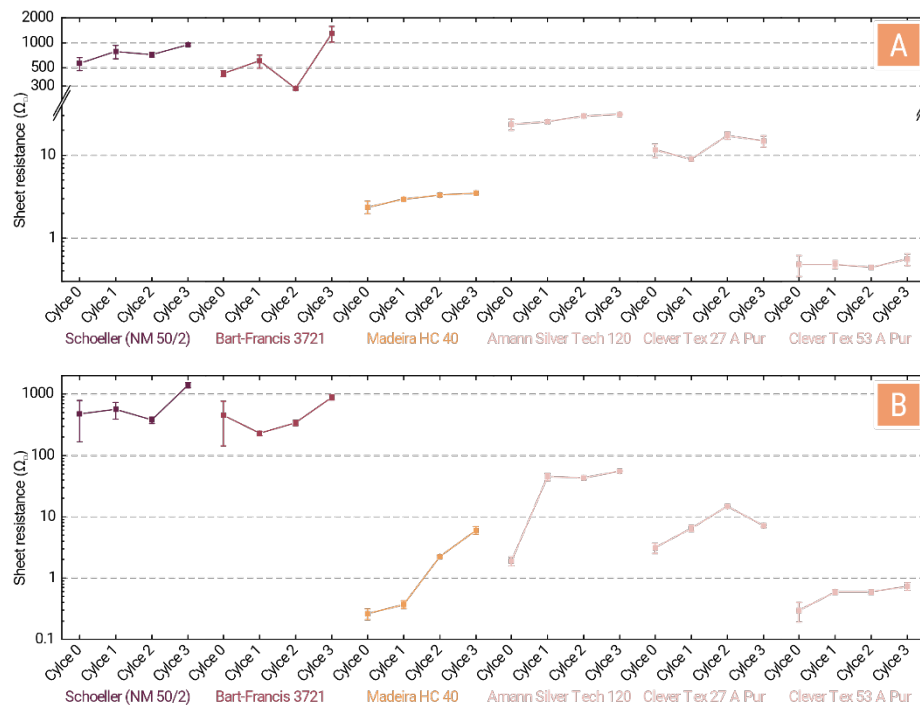


Fig. 9. Some of the evaluated yarns showed high sheet resistance, while others had very low resistance that remained stable even after three cycles. This stability was observed in samples measured both horizontally (A) and vertically (B).

Additionally, the removal of non-conductive layers during abrasion can expose conductive fibers, leading to a decrease in resistance. In some cases, the abrasion process may cause short circuits by unintentionally connecting different conductive sections, further lowering overall resistance. Another factor could be the sensitivity of the measuring instruments, which might detect improved conductive paths instead of damaged ones, especially if some pathways remain intact or improve. Lastly, abrasion can leave behind conductive debris, such as particles or fibers, that temporarily enhance conductivity despite visible damage. One cross-pattern sample, Clever Tex 27A PUR, completely broke after the second cycle, and no resistance could be measured.

For the visual inspection (cf. **Fig. 10. Close-up image of the 3rd cycle of abrasion with each yarn and pattern, where described effects are visible.**), the plain pattern is the most reliable with all yarns due to its higher contact points in the fabric. The twill pattern showed moderate durability, while the satin pattern caused significant pilling in all yarns; this could be due to the longer length of the yarn on the surface of the fabric. The cross pattern, known for its open geometry, demonstrated varied performance, with only a few yarns showing resilience. Madeira HC 40 exhibited strong durability, with the dense stitching of the plain pattern supporting its structure through multiple cycles. The twill pattern began to show loose ends after approximately 70 abrasion cycles, with some yarns performing better than others. The satin pattern caused significant wear on

Madeira HC 40 due to its exposed yarn loops. Although this yarn developed pilling, it still retained a relatively neat appearance compared to other yarns tested. Madeira HC 40 also performed reasonably well in the cross pattern, demonstrating good resilience in a challenging pattern. Schoeller NM 50/2, a spun yarn, initially showed good performance in the plain pattern, exhibiting minimal wear. However, its spun structure began to show pilling and minor short fibers as cycles progressed. This yarn's looser structure due to lower TPI was challenging for Schoeller NM 50/2, causing visible deterioration in its appearance. The open structure emphasized the yarn's weak points, making it one of the least suitable patterns for this spun yarn. Bart-Francis 3721, another spun yarn, performed reasonably well in the plain pattern, displaying some pilling but preserving structural integrity. Like Schoeller NM 50/2, Bart-Francis 3721 began showing damage in the twill pattern, with minor wear and loose ends becoming visible as cycles increased.

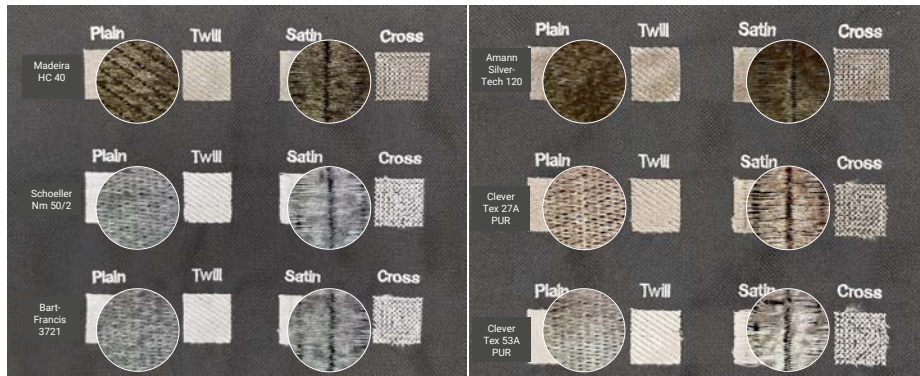


Fig. 10. Close-up image of the 3rd cycle of abrasion with each yarn and pattern, where described effects are visible.

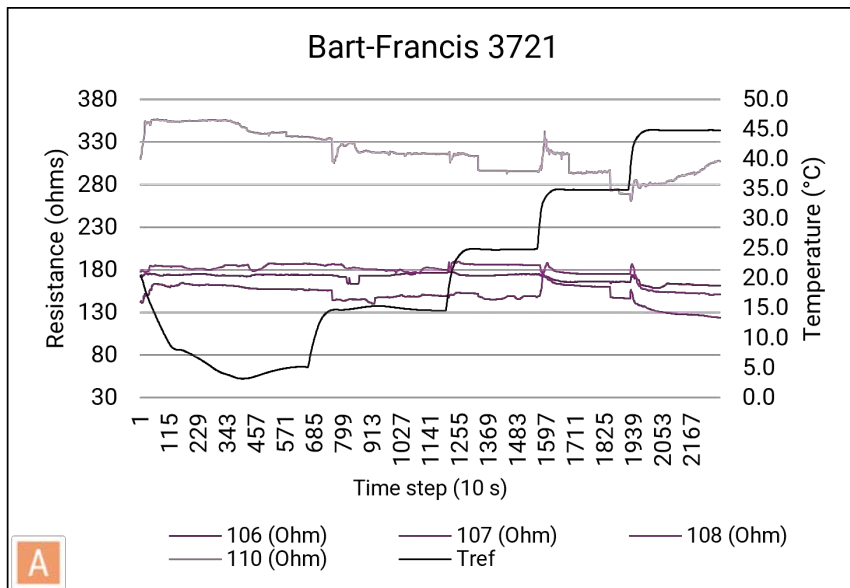
Amann Silver-Tech 120 consistently showed weak performance across all patterns due to its very loose structure. Despite the dense stitching, it showed significant wear and short fibers after just a few cycles, indicating its limited durability. Clever Tex 27A PUR performed well in the plain pattern, showing minimal wear even after multiple cycles. It was a moderate performer and slightly more prone to pilling in the satin pattern compared to the other good performers. Clever Tex 53A PUR was highly durable in the plain pattern, showing almost no signs of wear after extended abrasion cycles. Its compact structure effectively minimized loose ends. This yarn performed exceptionally well in the twill pattern, with minimal wearing and strong abrasion resistance. Even after prolonged cycles, the yarn retained its appearance. Although the satin pattern led to early pilling, Clever Tex 53A PUR held up better than most, showcasing its resilience. The long loops of the satin pattern were less damaging to this yarn compared to others. In the cross pattern, Clever Tex 53A PUR demonstrated good resilience, with only slight wear after the first cycles.

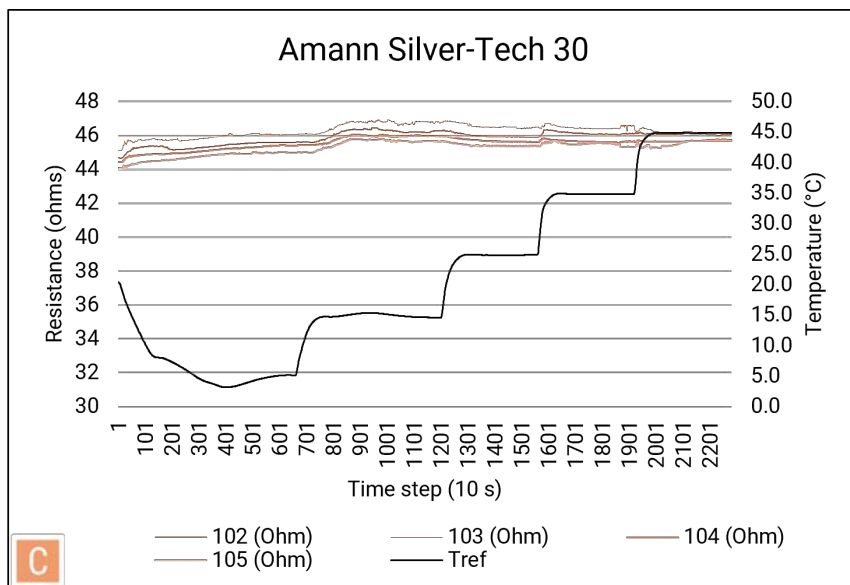
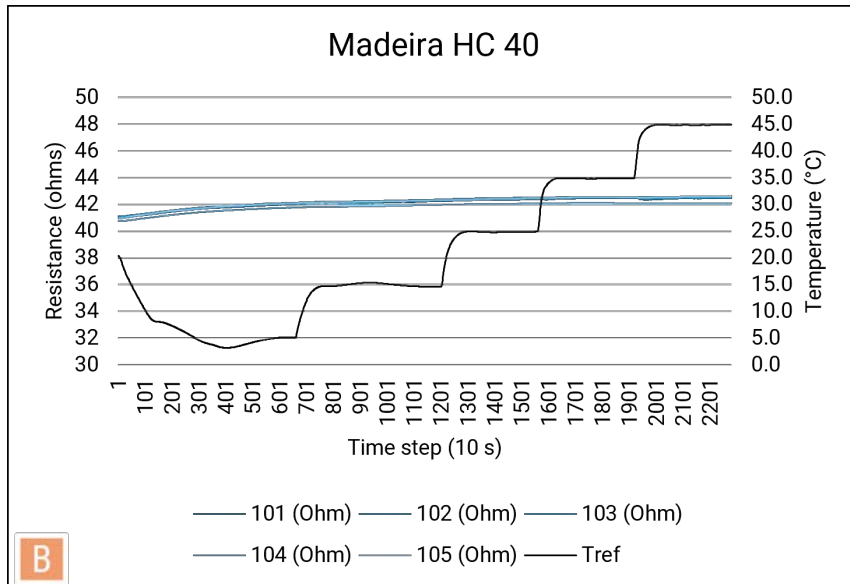
Both Madeira HC 40 and Clever Tex 53A PUR displayed the best durability across all patterns. Their compact structures and resistance to wear made them the most

durable yarns tested. The plain pattern appeared as the most durable across all yarns due to its higher stitching density. The twill pattern showed moderate durability, though spun yarns experienced loose ends. The satin pattern caused significant pilling in all yarns, with Clever Tex 53A PUR and Madeira HC 40 showing comparatively higher resistance. The cross pattern was the least durable, as its open geometry increased openness to damage; only Madeira HC 40 and Clever Tex 53A PUR demonstrated good strength. Overall, Madeira HC 40 and Clever Tex 53A PUR are recommended for applications requiring exceptional durability across various patterns, with the plain pattern being the most consistently reliable choice.

3.5 Wearability Test

Among the five materials tested, the resistance variation across the investigated temperature range was negligible for most samples, except for those fabricated with the Bart-Francis 3721 yarn. **Fig. 11** represents the resistance measurements from the 25 samples grouped by type of yarn used for fabrication, with the temperature profile recorded by the RTD inside the climate chamber displayed on the secondary axis.





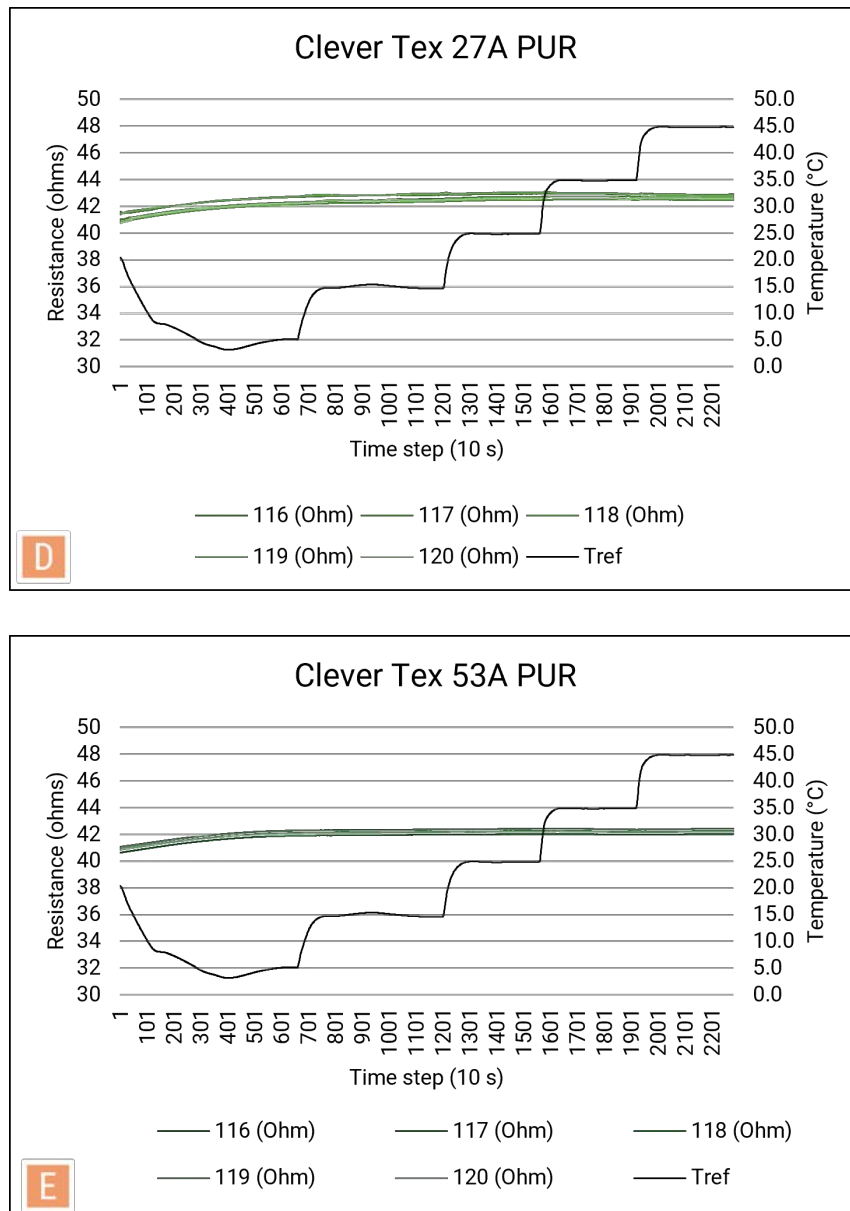


Fig. 11. Resistance tests were performed under thermal stress (F) for five materials: Bart-Francis 3721 (A), Madeira HC 40 (B), Amann Silver-Tech 30 (C), Clever Tex 27A PUR (D), and Clever Tex 53A PUR (E).

The resistance measured for the Ammax Silver-Tech 30 yarn (**Fig. 11, C**) ranges between 44 and 47 Ω across four samples, demonstrating minimal variation throughout

the temperature range. Similarly, the Madeira HC 40, Clever Tex 53A PUR, and Clever Tex 27A PUR yarns (**Fig. 11, D, and E**) exhibit resistance values between 41 and 43 Ω , indicating that resistance remains stable under varying temperature conditions and that the consistency across samples is high. In contrast, the Bart-Francis 3721 textile (**Fig. 11, A**) shows no clear correlation between resistance and temperature, with significant variability in resistance values across samples, ranging from 123 to 355 Ω , suggesting potential repeatability issues. To improve the interpretability of these results, the subplot resistance axes should be scaled appropriately to better reflect the spread of the data, enabling clearer detection of trends and variations, particularly for materials with high variability, such as the Bart-Francis 3721 yarn.

During the test, the environmental conditions were monitored and controlled by the HVAC system. The average air temperature was 22 °C, RH of 32 %, and air velocity 0.16 m/s. **Fig. 12** shows the resistance measurements together with the skin temperature. During the whole experiment, skin temperature averaged 25.0 ± 0.1 °C. The heat flux generated to maintain constant body temperature was strongly increased when switching from dry (~ 100 W m⁻²) to wet (~ 300 W m⁻²) conditions due to evaporative cooling. The tests performed on the manikin show consistent results related to the previous ones, reported in Figure 11. In dry conditions, all samples display resistances of around 40 Ω except for the Bart-Francis 3721 sample that, following previous tests, displays a much higher resistance (around 650 Ω). Sweating was activated after approximately 100 min (sample 590). During the transition from dry to wet operating mode, the Bart-Francis 3721 sample displayed a resistance drop to 160 Ω .

The Amann Silver Tech 30 sample showed an increase in resistance from 45 Ω to 47 Ω , while the remaining samples (Madeira HC 40, Clever Tex 27 A PUR, and Clever Tex 53 A PUR) displayed a constant resistance of 42 Ω throughout the experiment. It should be noted that the onset of the resistance variation might differ from sample to sample during the dry-to-wet transition, as samples might have been closer or farther from sweating pores.

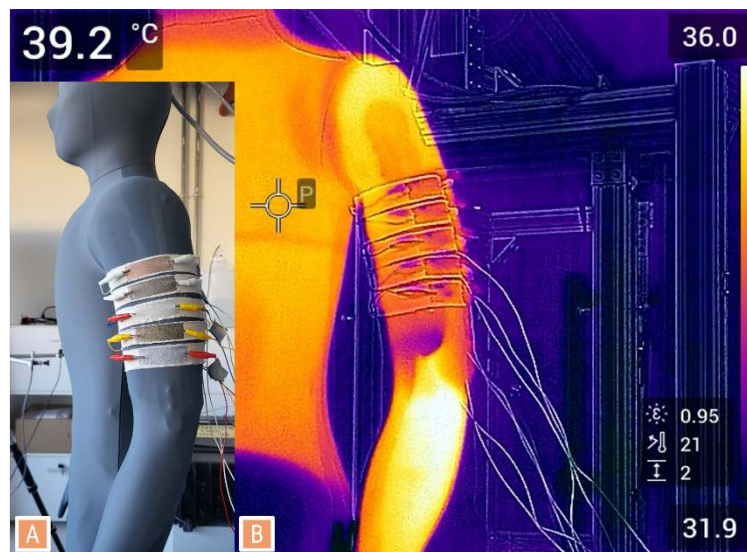
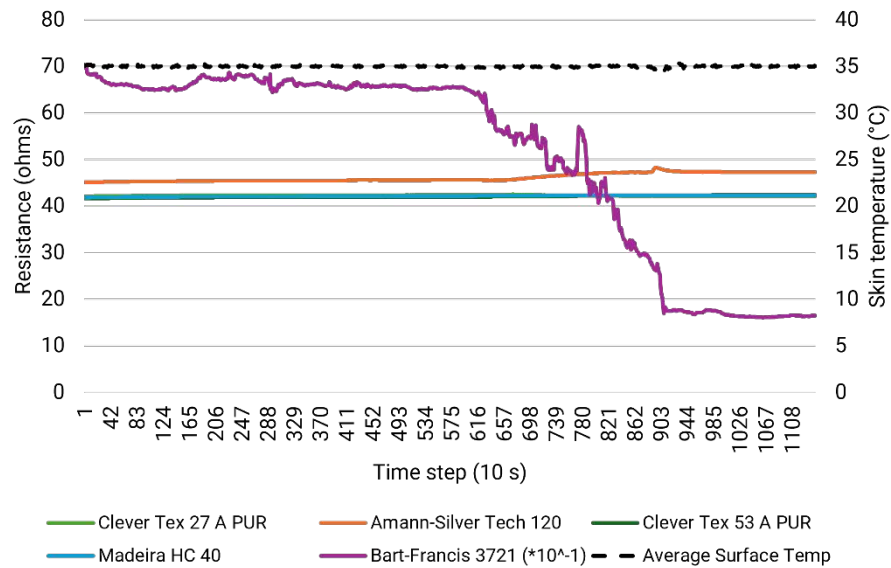


Fig. 12. Resistance tests were performed under dry and wet conditions for five materials (top). Setup overview (bottom) in dry mode (A), a thermal image of the manikin arm to show the surface temperature (B).

4 Discussion

The results demonstrate that yarn properties, including hairiness and thickness variations, significantly affect their performance. Yarns with lower hairiness and consistent structural integrity exhibited higher durability and electrical stability during embroidery-based testing. For instance, highly twisted yarns with lower hairiness improve durability in embroidery but may reduce flexibility, which is critical in knitted structures. This interplay of properties emphasizes the need for application-specific optimization. Furthermore, while this research focused on controlled laboratory conditions, real-world wear scenarios introduce additional complexities. Factors such as repeated washing, exposure to environmental parameters (moisture, temperature fluctuations), and prolonged mechanical strain can alter the electrical and mechanical properties of the yarn. These challenges underline the importance of further testing under realistic conditions to ensure reliable long-term performance. The interdisciplinary nature of smart textiles also plays a crucial role in yarn selection. Different applications ranging from healthcare to athletic wear and interactive garments demand specific characteristics, such as stretchability for movement tracking or high conductivity for heating textiles. The study reinforces the necessity of understanding the interaction between yarn properties and manufacturing techniques. For instance, embroidery, knitting, and weaving impose unique mechanical stresses that influence the conductive pathways and overall sensor performance. These insights complement the existing literature and emphasize the importance of selecting conductive yarns based on specific parameters that influence their performance in real-world applications.

Overall, the study provides a foundational framework for selecting and optimizing conductive yarns in smart textile design. Future work should focus on expanding the scope of testing to include real-world stress conditions and integrating advanced characterization techniques, such as strain monitoring, to capture dynamic property changes during use. Such advancements will enable researchers and designers to further refine conductive yarn applications, paving the way for more robust and versatile smart textiles.

5 Conclusion and Future Work

In this paper, a comprehensive evaluation of commercially available conductive yarns for their suitability in smart textile applications was conducted, focusing on critical factors such as durability, resistance consistency, and performance under various stress conditions. Through detailed analyses of yarn characteristics such as hairiness, thickness irregularities, and simulated wear tests, this study outlines a structured methodology for assessing and selecting optimal yarns for integration into textile-based wearable applications. Notably, yarns with minimal hairiness demonstrated superior resilience and electrical stability, highlighting the importance of structural consistency and durability in achieving reliable performance in smart textile applications. As the field of smart textiles is highly interdisciplinary, with researchers from diverse backgrounds working on various applications, understanding the fundamental parameters

that guide yarn selection for specific requirements is crucial. This study contributes to this understanding by presenting a framework for evaluating conductive yarns. However, it is important to acknowledge the limitations of the research. While testing conditions were carefully controlled, they do not fully replicate real-world wearing scenarios where multiple stress factors, such as prolonged mechanical strain, occur simultaneously. These factors could impact yarn performance in ways not captured in this study. Moreover, the study primarily focuses on embroidery-based techniques, and the findings must be adapted for other textile manufacturing methods, such as weaving and knitting, which involve different mechanical and structural challenges. Future research should aim to validate the proposed methodology under realistic wear conditions and explore the application of the findings across various smart textile production techniques to ensure broader applicability. This understanding will further enable researchers to make informed decisions in selecting and optimizing conductive yarns for diverse smart textile applications.

Acknowledgment

This work was funded by Tratter Engineering and the European Union Next-Generation EU (Piano Nazionale di Ripresa e Resilienza, PNRR - DM 117/2023). This work was also supported by the Autonomous Province of Bozen-Bolzano-South Tyrol's European Regional Developmental Fund (ERDF) Program under Project EFRE/FESR 1011-SmartCover and under Project EFRE/FESR 1007 iPlayground. This manuscript reflects only the authors' views and opinions, neither the European Union nor the European Commission can be considered responsible for them.

References

1. R. De Fazio, V. M. Mastronardi, M. De Vittorio, and P. Visconti, "Wearable Sensors and Smart Devices to Monitor Rehabilitation Parameters and Sports Performance: An Overview," *Sensors*, vol. 23, no. 4, p. 1856, Feb. 2023.
2. S. Yasuhiro and J. Lei, "Motion Capture Glove: An Intuitive Wearable Input Device," in 2018 IEEE 7th Global Conference on Consumer Electronics (GCCE), Oct. 2018.
3. M. Stoppa and A. Chiolerio, "Wearable electronics and smart textiles: a critical review," *Sensors (Basel)*, vol. 14, no. 7, pp. 11957–11992, Jul. 2014.
4. Y. Zheng et al., "Performance evaluation of conductive tracks in fabricating e-textiles by lock-stitch embroidery," *Journal of Industrial Textiles*, vol. 51, no. 4_suppl, pp. 6864S–6883S, Jun. 2022.
5. S. U. Zaman, X. Tao, C. Cochrane, and V. Koncar, "Understanding the Washing Damage to Textile ECG Dry Skin Electrodes, Embroidered and Fabric-Based; set up of Equivalent Laboratory Tests," *Sensors*, vol. 20, no. 5, p. 1272, Feb. 2020.
6. S. Uz Zaman, X. Tao, C. Cochrane, and V. Koncar, "Laundryability of Conductive Polymer Yarns Used for Connections of E-textile Modules: Mechanical Stresses," *Fibers Polym*, vol. 20, no. 11, pp. 2355–2366, Nov. 2019.
7. M. N. Warncke et al., "Novel functional and fail-safe knitted heating structures via the dedicated serial-parallel circuits for heating design approach," *Textile Research Journal*, vol. 94, no. 5–6, pp. 725–739, Mar. 2024.

8. Y. Chen, J. Hart, M. Suh, K. Mathur, and R. Yin, "Electromechanical Characterization of Commercial Conductive Yarns for E-Textiles," *Textiles*, vol. 3, no. 3, pp. 294–306, Aug. 2023, doi: 10.3390/textiles3030020.
9. R. K. Raji, X. Miao, and A. Boakye, "Electrical Conductivity in Textile Fibers and Yarns—Review," *AATCC Journal of Research*, vol. 4, no. 3, pp. 8–21, May 2017, doi: 10.14504/ajr.4.3.2.
10. J. Mersch *et al.*, "Integrated Temperature and Position Sensors in a Shape-Memory Driven Soft Actuator for Closed-Loop Control," *Materials*, vol. 15, no. 2, p. 520, Jan. 2022, doi: 10.3390/ma15020520.
11. L. Hao, Z. Yi, C. Li, X. Li, W. Yuxiu, and G. Yan, "Development and characterization of flexible heating fabric based on conductive filaments," *Measurement*, vol. 45, no. 7, pp. 1855–1865, Aug. 2012, doi: 10.1016/j.measurement.2012.03.032.
12. Y. Wang, W. Yu, and F. Wang, "Structural design and physical characteristics of modified ring-spun yarns intended for e-textiles: A comparative study," *Textile Research Journal*, vol. 89, no. 2, pp. 121–132, Jan. 2019.
13. A. Shahzad *et al.*, "Processing of metallic fiber hybrid spun yarns for better electrical conductivity," *Materials and Manufacturing Processes*, vol. 34, no. 9, pp. 1008–1015, Jul. 2019.
14. M. Amin, M. Ullah, and A. Akbar, "Identification of Cotton Properties to Improve Yarn Count Quality by Using Regression Analysis," 2014. Accessed: Nov. 15, 2024. [Online]. Available: <https://www.semanticscholar.org/paper/Identification-of-Cotton-Properties-to-Improve-Yarn-Amin-Ullah/6e865111ec6e6fdde8486efee26b7bd38566ac25>
15. Y. Liu *et al.*, "Enhancing the Spun Yarn Properties by Controlling Fiber Stress Distribution in the Spinning Triangle with Rotary Heterogeneous Contact Surfaces," *Polymers*, vol. 15, no. 1, p. 176, Dec. 2022.
16. N. Haleem and X. Wang, "A comparative study on yarn hairiness results from manual test and two commercial hairiness metres," *Journal of The Textile Institute*, vol. 104, no. 5, pp. 494–501, May 2013.
17. V. H. Carvalho, P. J. Cardoso, R. M. Vasconcelos, F. O. Soares, and M. S. Belsley, "Optical Yarn Hairiness Measurement System," in 2007 5th IEEE International Conference on Industrial Informatics, Jun. 2007, pp. 359–364.